BIOMASS Forest Height Product ATBD

Ref: BIO-BPS-FH-ATBD-ARE-10343
Issue: 2.2.0
Date: 13/03/2026

Document information

Title	BPS FH ATBD - Algorithms Theoretical Baseline Document
Internal Ref.	
External Ref.	BIO-BPS-FH-ATBD-ARE-10343
Date	13/03/2026
Issue	2.2.0
Pages	45

Recipients	
Cristiano Lopes	ESA – ESRIN
Michele Caccia	ESA – ESRIN
Muriel Pinheiro	ESA - ESRIN

Prepared by	
Francesco Banda	Aresys
Kostas Papathanassiou	DLR
Paolo Mazzucchelli	Aresys
Riccardo Piantanida	Aresys
Laurent Ferro-Famil	ISAE-SUPAERO, CESBIO

Checked by	
Davide D’Aria	Aresys

Approved by	
Davide D’Aria	Aresys

Change history

Date	Issue	Change	Author
09/06/2022	2.0	First issue of the document.	Francesco Banda Review: Kostas Papathanassiou
28/10/2022	2.1	CDR2 issue of the document • BPSPDR2-14: Processing Parameters clarified (Sec. 4.1.4) • BPSPDR2-18, BPSPDR2-27, BPSPDR2-28, BPSPDR2-30: ATBD revised according to guidelines • BPSPDR2-23: RVOG Reflectivity profile clarified (Sec. 3.4.2) • BPSPDR2-24: editorials amended • BPSPDR2-32: solved TBD/TBC in delivery pack • BPSPDR2-54: uncertainty threshold clarified (Sec. 3.4.4) • BPSPDR2-72: Hectare amended • BPSPDR2-74: Inputs and outputs dimensions clarified • BPSPDR2-75: number clarified (Sec. 4.1.4) • BPSPDR2-78: Vertical reflectivity profiles clarified (Sec. 3.4.2) • BPSPDR2-83: documents review to enforce consistency • BPSPDR2-84: Revision of re-use of backgeocoding results at L2 (Sec. 3.2) • BPSPDR2-86: Computation of spatial average window size clarified (Sec. 3.3.4) • BPSPDR2-87: Cross-pol terminology aligned • BPSPDR2-88: Incidence angle clarified (Sec. 3.3.4) • BPSPDR2-89: FH quality index revised (Sec. 4.1.4)	Francesco Banda Review: Kostas Papathanassiou Paolo Mazzucchelli
13/03/2022	2.1.1	Post CDR2 issue of the document: • BPSCDR2-3: added docs acronyms in i/o tables • BPSCDR2-4: added missing details for Forest Cov Check • BPSCDR2-8: updated section 3.4.2 • BPSCDR2-10: vertical datum/reference added section 3.6.4.1.1 • BPSCDR2-13: updated section 2.3.1 • BPSCDR2-14: note added section 3.3.2 • BPSCDR2-16: note added section 3.4.4.3 • BPSCDR2-18: section 3.5.2 rephrased to be crystal clear • BPSCDR2-19: section 3.5.4.1.2 note added • BPSCDR2-20: section 3.5.4.1.3 note added • BPSCDR2-21: updated section 3.5.4.1.5 • BPSCDR2-22: updated section 3.6.4.1.2 • BPSCDR2-23: note added section 3.4.4 • BPSCDR2-30: Heat Map added section 4.1.4	Paolo Mazzucchelli Kostas Papathanassiou Francesco Banda Laurent Ferro-Famil

Date	Issue	Change	Author
		• BPSCDR2-43: minimum coverage percentage added section 4.1.4 • BPSCDR2-45: configuration added section 3.5.2 • Wavenumber LUT dimension decoupled from height dimension: updated section 3.5.2 • Feathering added at L2B: updated section 4 • Formulas corrected: updated section 3.4.4 • Ground to volume ratio configuration updated: updated section 3.5	
15/09/2023	2.1.2	BPS-393 / BPS-392: added notes on FH inversion algorithm efficient implementation.	Paolo Mazzucchelli
19/1/2024	2.1.3	DeltaFAT2 version of the document: • BPSCDR2-10: updated description of “real elevation”	Paolo Mazzucchelli
17/520/24	2.1.4	Post DeltaFAT2 version of the document: • updated default values to avoid data masking • modified relations 3.12, 3.13 • updated equation 3.2 • added TBD/TBC table	Paolo Mazzucchelli
06/09/2024	2.1.5	FAT3 version of the document	Paolo Mazzucchelli
13/12/2024	2.1.6	Delta_FAT3 version of the document: • updated section 3.4.5 • renamed “decimationFactor” to “upsamplingFactor”	Paolo Mazzucchelli
07/03/2025	2.1.7	Post-FAT3 issue of the document Fixed Wavenumbers (3.4.2), IncidenceAngle and Terrain Slope (3.5.2) descriptions unit of measurement	Paolo Mazzucchelli
30/04/2025	2.1.8	BPS-FTO-BATCH4: Separated calibration screen table in skp and flattening (section 3.3.2); expanded description in how to use them (section 3.3.4)	Paolo Mazzucchelli Emanuele Giorgi
13/03/2026	2.2.0	Post-launch issue of the document (associated to BPS V4.4.0) • 3.4.4.3. Coherence calibration: removed cos(incidence angle) term	Paolo Mazzucchelli Emanuele Giorgi

Table of contents

1. Introduction

1.1. Context

BIOMASS is ESA's 7th Earth Explorer mission. The purpose of the BIOMASS is to reduce the uncertainty in the worldwide spatial distribution and dynamics of forest biomass in order to improve current assessments and future projections of the global carbon cycle. This objective will be achieved by the implementation of a P-band SAR mission, providing global maps of forest biomass stocks, forest disturbance and growth.
The BIOMASS mission will also provide 3D views of forests through the "tomographic" phase and will also support additional science needs arising from the opportunity to explore the Earth for the first time with a P-band SAR system from space offering the possibility to "see" below the vegetated areas and in beneath bare soil or icy regions.

To achieve its challenging objectives, the BIOMASS mission requires a specific data processing strategy that combines different technologies at different processing level in order to generate the final Above Ground Biomass global map.

1.2. Scope of the document

The purpose of this document is to provide the "Forest Height Algorithms Theoretical Baseline Document (ATBD)" for the BIOMASS Processing Suite (BPS) project.
This document is organized as follows:

- Section 1: Overview of the document;
- Section 2: Brief introduction about BPS and Forest Height processing;
- Section 3: Description of L2a Forest Height algorithms;
- Section 4: Description of L2b/L3 Forest Height algorithms.

1.3. Acronyms

Acronym	Description
AD	Applicable Document
ADS	Annotation datasets
AGB	Above Ground Biomass
ARESYS	Advanced Remote Sensing and Systems
ATBD	Algorithm Theoretical Baseline Document
AUX	Auxiliary
BIODEMPP	Biomass DEM Prototype Processor

Acronym	Description
BPS	BIOMASS Processing Suite
CM	Covariance Matrix
CFI	Customer Furnished Items
CoSCS	Coregistered SCS
CP	co-polarization
DEM	Digital Elevation Model
DGG	Discrete Global Grid
DTM	Digital Terrain Model
ECSS	European Cooperation for Space Standardization
EO-CFI	Earth Observation Custom Furnished Items
ESA	European Space Agency
GPP	Ground Processor Prototype
GPS	Global Positioning System
FD	Forest Disturbance
FH	Forest Height
FNF	Forest/Non-Forest Mask
IERS	International Earth Rotation Service
InSAR	Interferometric Synthetic Aperture Radar
INT	Interferometric Phase
L0	Level-0 product
L1c	Level-1c product
L2a	Level-2a product
L2b	Level-2b product
L3	Level-3 product
LOS	Line Of Sight
LUT	Look-Up Table
PF	Processing Facility
PFD	Product Format Specification Document
RD	Reference Document
SAR	Synthetic Aperture Radar
SCS	Single-look Complex Slant-range
SKP	Sum of Kronecker Products
SNR	Signal-to-Noise Ratio

Acronym	Description
TBD	To Be Defined
TBC	To Be Confirmed
TOM	Tomographic Phase
XML	eXtended Markup Language
XP	cross-polarization

1.4. TBD / TBC Table

Section	TBD / TBC	Page
1.6	BTK_WEB: link must be defined	9

1.5. Applicable documents

[AD1] BIOMASS Production Model, BIO-ESA-EOPG-EEGS-TN-0046, issue 3.5
[AD2] BIO-BPS-L1-PFD, BIOMASS L1a,b,c products format specification, I/R 1/2/2
[AD3] BIO-BPS-TN-PRODMOD, BIOMASS Production Model Technical Note, I/R 1/2/1

1.6. Reference documents

[RD1] BIO-BPS-L1-STACK-ATBD, BIOMASS BPS L1c Stack ATBD, I/R 1/1/2
[RD2] BIO-BPS-L1-SAR-ATBD, BIOMASS BPS L1 SAR ATBD, I/R 1/1/2
[RD3] BIOMASS DEM Product Processor Prototype, DEM Processor Algorithm Theoretical Baseline Document, BIODEMPP-CoSCS-DEM-01, I/R 4/0
[RD4] BIO-BPS-FD-ATBD, BIOMASS BPS FD ATBD, I/R 2/1/1
[RD5] BIOMASS L2 Implementation Study ATBD, I/R 1/5
[RD6] F. Kugler, S. Lee, I. Hajnsek and K. P. Papathanassiou, "Forest Height Estimation by Means of Pol-InSAR Data Inversion: The Role of the Vertical Wavenumber," in IEEE Transactions on Geoscience and Remote Sensing, vol. 53, no. 10, pp. 5294-5311, Oct. 2015
[RD7] BIO-BPS- AUX-FMT, BPS Auxiliary Product Format, I/R 2/1/1
[RD8] BIO-BPS-PPD, BIOMASS BPS Product Performance Description, I/R 2/0/2
[RD9] F. Kugler, D. Schulze, I. Hajnsek, H. Pretzsch and K. P. Papathanassiou, "TanDEM-X Pol-InSAR Performance for Forest Height Estimation," in IEEE Transactions on Geoscience and Remote Sensing, vol. 52, no. 10, pp. 6404-6422, Oct. 2014
[RD10] R. Guliaev, V. Cazcarra-Bes, M. Pardini and K. Papathanassiou, "Forest Height Estimation by Means of TanDEM-X InSAR and Waveform Lidar Data," in IEEE Journal of Selected Topics in Applied Earth Observations and Remote Sensing, vol. 14, pp. 3084-3094, 2021

[RD11] Y. Cui, Y. Yamaguchi, H. Yamada and S. Park, "PolInSAR Coherence Region Modeling and Inversion: The Best Normal Matrix Approximation Solution," in IEEE Transactions on Geoscience and Remote Sensing, vol. 53, no. 2, pp. 1048-1060, Feb. 2015

[RD12] BIOMASS L2 Implementation Study ARD, I/R 2/7

[RD13] BIO-BPS-IODD, BIOMASS BPS IODD, I/R 1/1/3

[RD14] Pinheiro, M.; Amao-Oliva, J.; Scheiber, R.; Jaeger, M.; Horn, R.; Keller, M.; Fischer, J.; Reigber, A. Dual-Frequency Airborne SAR for Large Scale Mapping of Tidal Flats. in Remote Sens., vol. 12, pag. 1827, 2020

[RD15] BTK_WEB, official link: TBD

2. BPS and FH Processing Overview

2.1. BPS Overview

The BIOMASS Processing Suite (BPS) is in charge of processing BIOMASS Level-0 data up to Level-3, generating a wide set of products. Product generation scheme is depicted in the following two figures respectively for the TOM phase and INT phase. The processing foresees the following steps:

- **L1 processing**: the BIOMASS image formation step, taking in input 1 L0 slice and generating in output N>=1 L1 frames;
- **Stack Processing**: the coregistration and stacking processing step that will define the required 7-images Tomographic stacks or the 3-images Interferometric stacks. It includes stack phase calibration;
- **L2a Processing**: processing step for each stack that provides the inputs to the further products Tile Generation performed by the L2b processors. For one global cycle the number of stacks varies mainly with latitude, approximately from a minimum of two at the Equator (ascending/descending) to about six at higher latitudes (three ascending/descending pairs);
- **L2b Processing**: processing that aggregates all the stack-based L2a products insisting on the same location on ground (Tile) in the same time interval and generates a single BIOMASS L2b product. A different number of stacks may be available for each DGG tile [RD8], based on tile dimensions and swath coverage (which is not related to DGG tiling pattern);
- **L3 Processing**: consolidation processing removing discontinuities in L2b products.

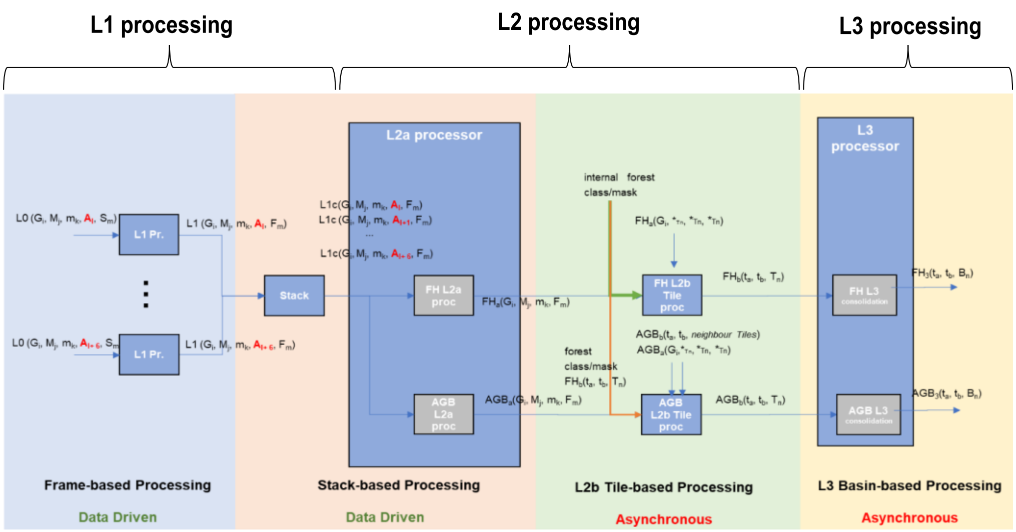

Fig.1 Biomass high-level processing scheme from L0 data to L3 products, TOM phase.

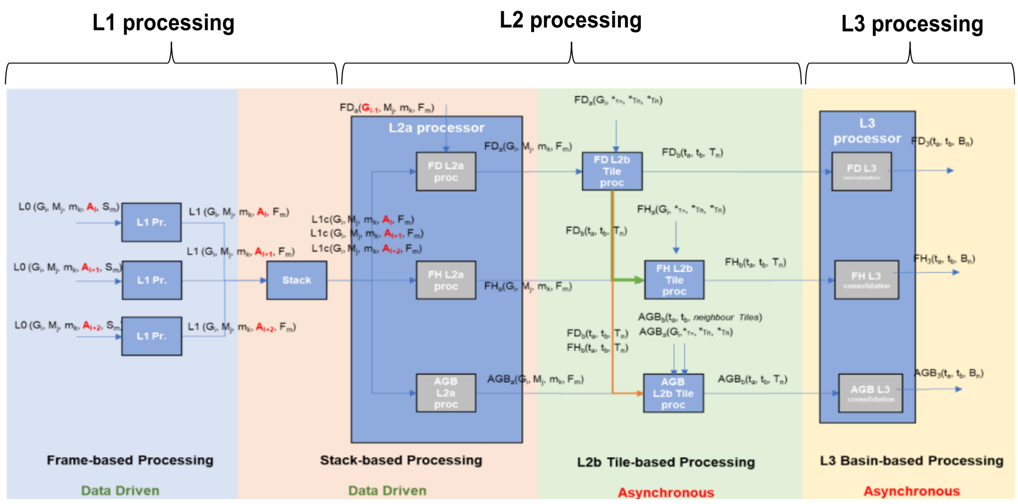

Fig.2 Biomass high-level processing scheme from L0 data to L3 products, INT phase.

2.2. FH Processing Overview

The FH processing has as main goal the generation of maps of forest height at a spatial resolution roughly equivalent to ~200 m x 200 m (i.e. 4 ha) at the Equator [RD5]. It receives as input a stack of BIOMASS Level-1c images (SCS co-registered and calibrated stack), including its relevant annotated data [AD2]. Same algorithms are envisaged to generate the same product in INT and TOM phases. The FH processing is divided into three levels:

- L2a, generates a map of forest height from each L1c stack based on model inversion algorithm, as well as a quality map;
- L2b, generates a forest height map merging all the L2a products on a geographic grid tile, as well as an updated quality map;
- L3, consolidates the result removing discontinuities in L2b products.

NOTE: L3 processing currently does not entail any additional step with respect to L2b. This will be confirmed/reassessed at future milestones. For the moment L3 is kept as a placeholder for eventual future evolutions. Eventually, L2b can be an empty container and the product will be copied to L3.

NOTE: Provided that FD algorithm proper validation will only be possible with BIOMASS in orbit, the strategy proposed to deal with FH/AGB dependency on FD is to initially input to FH/AGB a forest/non-forest mask generated outside of BPS [AD1] [AD3]. After testing FD performance with BIOMASS in orbit, FD dependency can be switched on again, provided it has a satisfactory performance. The diagram of Fig.2 reports nonetheless FD input for completeness.

NOTE: L2 processor receives from Stack processor L1c products with two co-polarization (CP) channels and one cross-polarization (XP) channel. Details on the aggregation of XP channels into one XP are reported in [RD1].

NOTE: Regarding stack images cardinality, their number can vary (not always 3 or 7) due to contingency reasons and it can go up to 8 in TOM phase.

2.3. FH Processing Workflow and Algorithmic Overview

The main steps of FH processing workflow are depicted in the following figure and described in detail in the following sub-sections.

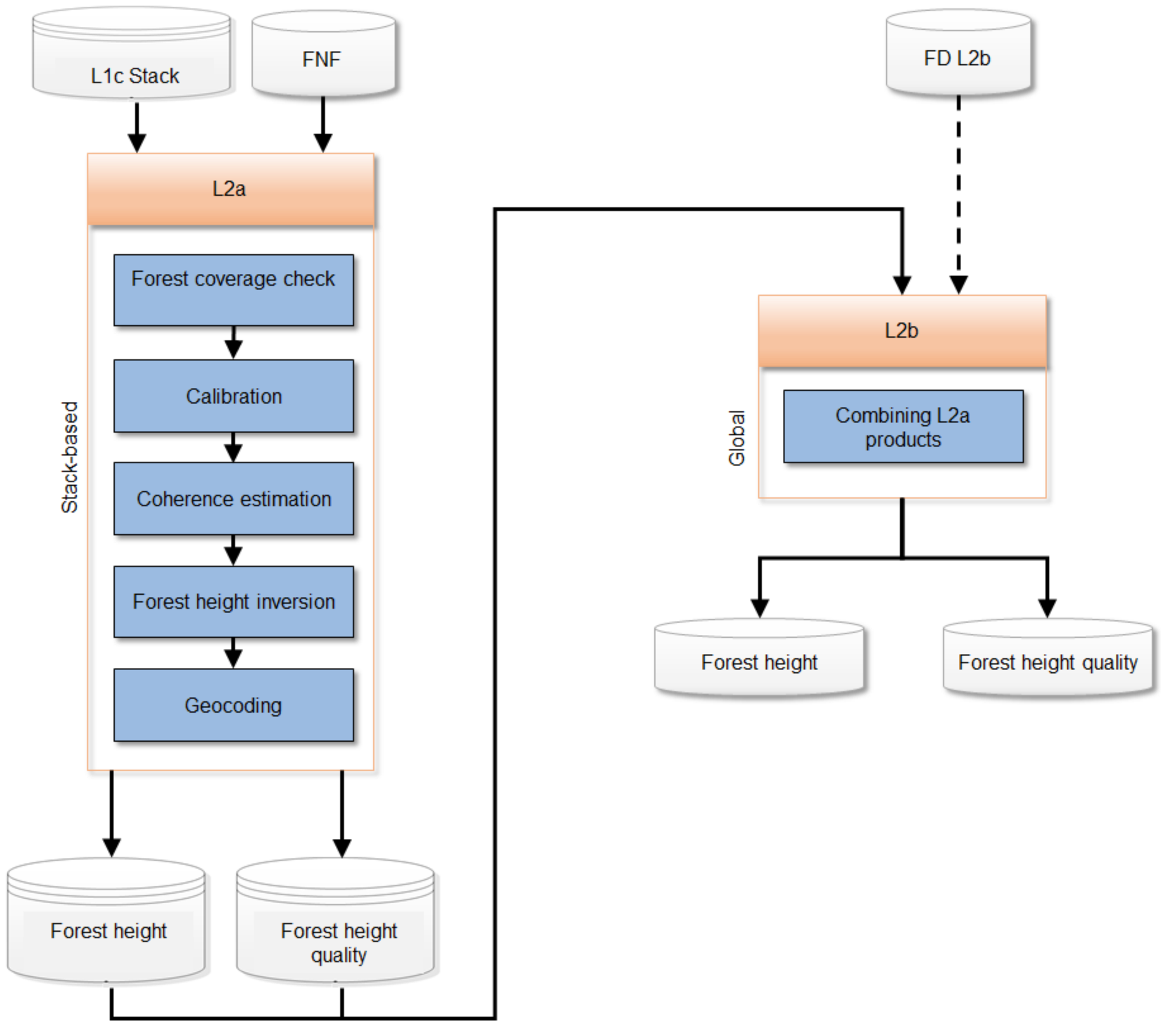

Fig.3 FH processing detailed workflow.

2.3.1. Forest height (L2A_P)

The main steps of the stack-based L2a block are:

- forest coverage check: predetermine which input data (as a whole image) should need to be processed;
- calibration: application of phase calibration and ground steering (terrain at zero elevation) screens to the stack;
- coherence estimation: computes the polarimetric-interferometric coherence matrix from data and compensates non-volumetric decorrelation;
- forest height inversion: fit of the model to computed coherences, generates a map of forest height as well as a quality map;
- geocoding: projects the processed data on geographic map, accounting for the different forest points location with respect to reference DEM.

2.3.2. Forest height aggregation (L2B_FH_P)

The main steps of the L2b block are:

- combining: fusion of L2a estimates at map level.

2.3.3. Note on interpretation of inputs and outputs tables

Inputs and outputs for each processing sub-step are summarized in specific subsections (two subsections for each substep). A specific tabular format is defined to improve the access to the document. The meaning of each column is exemplified in the following table.

Symbol	Name	Origin/ Destination	Size	Variability	Default	Description
Mathematical symbol of the quantity appearing in formulas.	Name of the quantity as related to other BPS documentation (e.g., AUX_FMT, L1 ATBDs, …)	BPS document name describing the origin of the quantity or processing step of origin/destination or BPS product of destination.	Dimensions of the quantity.	Range of values or update rate of an internal resource.	Default value for configuration parameters.	Verbal description of the quantity and its characteristics (e.g. measure units, …)

3. Forest height

The overall scheme of the L2a processing is reported in Fig.3.
The key steps are coherence estimation and the forest height inversion. These steps are described in detail in the following subsections.

3.1. Forest Coverage Check

3.1.1. Overview and rationale

The availability of a general FNF map allows to predetermine which input data (as a whole image) should need to be processed. A threshold (*mF*) must be set as input parameter to select the minimum forest coverage (as a percentage of the whole area covered by the images) to start or skip computation.

The step is optional.

3.1.2. Inputs

Symbol	Name	Origin	Size	Variability	Default	Description
FNF	FNF	Internal resource (IODD)	$[N_{lat,FNF} \times N_{lon,FNF}]$	Yearly	-	A global forest-non-forest mask given as input
mF	forestCoverageThreshold	AUX_PP2_2A (AUX_FMT)	float value [scalar]	0.0-100.0	5.0	The minimum [%] relative forest coverage that triggers the computations
BB	Footprint	L1c main product header (L1_PFD)	lat-lon vertices (4 couples)	-	-	The extent of the L1c input data in geographical coordinates

3.1.3. Outputs

Symbol	Name	Destination	Size	Variability	Default	Description
TR	trigger	*Next steps*	Boolean [scalar]	-	True	Allows to trigger (True) the computation of the change detection

3.1.4. Algorithm mathematical background

The values of the FNF mask that lie within the area covered by the image, defined by the bounding box *BB*, are extracted from the global FNF mask. The relative number of forested pixels is compared to the required minimum threshold *mF* to trigger any subsequent computation.

$$TR = \left(100 * \frac{ForestedArea|_{BB}}{TotalArea|_{BB}} > mF\right) \quad (3.1)$$

3.1.5. Notes on implementation

The substep should be as fast as possible, as its unique role is to avoid any un-useful computation. Thus, comparison is carried on at the original FNF mask spatial sampling (i.e. no reprojection needed), as any resampling does not have any impact on the relative percentage of forested area with respect to the total covered area. It must be noted that any noValue pixel in FNF is treated as ForestedArea sample to avoid skipping computation because of the presence of noValues in FNF.

Details on the derivation of external FNF are reported in [RD13].

3.2. INT subsetting (TOM only)

3.2.1. Overview and rationale

The algorithm applies only to TOM stacks and subsets the stack in order to select the acquisitions to operate as in INT phase. The only rule applicable at the moment follows a geometric criterion. Other rules could be defined post-launch.
This step is mandatory for TOM only.

3.2.2. Inputs

Symbol	Name	Origin	Size	Variability	Default	Description
SCS	L1c	Stack processor (L1_PFD)	M, each acquisition $[N_{rg} \times N_{az}]$	M=7/8 acquisitions (TOM phase), with two CP and one XP	-	L1c stack
-	subsettingRule	AUX_PP2_2A (AUX_FMT)	String	-	“geometry”	Select 3 acquisitions from the 7/8 of TOM phase, choosing, with a

Symbol	Name	Origin	Size	Variability	Default	Description
						geometrical rule, the baselines correspondin g to the ones of INT phase.

3.2.3. Outputs

Symbol	Name	Destination	Size	Variability	Default	Description
SCS	L1c	*Calibration step*	M, each acquisition $[N_{rg} \times N_{az}]$	M=3 acquisitions, with two CP and one XP	-	L1c stack

3.2.4. Algorithm mathematical background

3.2.4.1. Geometry criterion

The "geometry" criterion for subsetting selects among the seven/eight TOM stack the three acquisitions that give nominally consistent baselines with INT phase. As different combinations are possible, see Fig.4, the default rule is to select the central combination, which is corresponding to exactly the same nominal situation as INT. In case this combination presents a missing acquisition, the rule is to then evaluate remaining combinations in sequential order until a three-acquisitions combination is found. If no combination of three exists, the minimum required is two and the maximum baseline is equivalent to double TOM spacing. The contingency case with eight TOM acquisitions is reported in Fig.5.

```
                    0    1    2    3    4    5    6          TOM stack
Evaluation order    *    *    *    *    *    *    *
           2        *         *         *
           1             *         *         *               <-default
           3                  *         *         *
```

Fig.4 Selection for seven TOM.

```
                    0    1    2    3    4    5    6    7     TOM stack
Evaluation order    *    *    *    *    *    *    *    *
           2        *         *         *
           1             *         *         *               <-default
           3                  *         *         *
           4                       *         *         *
```

Fig.5 Selection for eight TOM (contingency).

3.3. Calibration

3.3.1. Overview and rationale

The calibration algorithm makes use of the L1c annotation [AD2] to apply phase calibration to L1c necessary for the L2a processing.

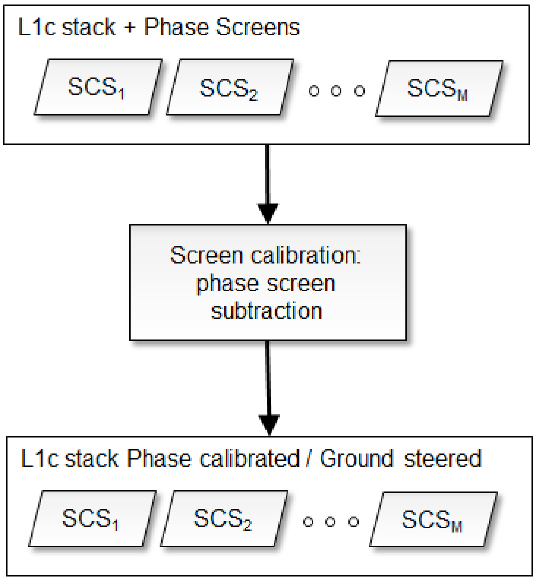

Fig.6 Calibration.

The step is mandatory. If disabled for debug, default rule is to copy inputs as step output.

3.3.2. Inputs

Symbol	Name	Origin	Size	Variability	Default	Description
SCS	L1c	Stack processor, or *INT subsetting step*	M, each acquisition $[N_{rg} \times N_{az}]$	M=3* acquisitions with two CP and one XP	-	L1c stack
φ_{skp}	skpCalibrationPhasesScreen	L1c reference acquisition ADS (L1_PFD)	M, each $[N_{rg,\varphi} \times N_{az,\varphi}]$ (zero for reference acquisition)	-	-	SKP calibration phase screens [rad]
$\varphi_{flattening}$	flatteningPhasesScreen	L1c reference acquisition ADS (L1_PFD)	M, each $[N_{rg,\varphi} \times N_{az,\varphi}]$ (zero for reference acquisition)	-	-	Ground steering (flattening) geometry phase screens [rad]
-	applyCalibrationScreen	AUX_PP2_2A (AUX_FMT)	string	'skp', 'geometry', 'none'	skp	Choose the phase calibration to be performed: skp or geometry if phase screens calibration should be applied, none otherwise.

*The nominal case is M=3 acquisitions, but the algorithm works also in contingency case when M=2

3.3.3. Outputs

Symbol	Name	Destination	Size	Variability	Default	Description
SCS	L1c	*Ground cancellation processing step*	M, each acquisition $[N_{rg} \times N_{az}]$	M=3 acquisitions with two CP and one XP	-	Phase calibrated and ground steered (terrain at zero level) L1c stack

3.3.4. Algorithm mathematical background

This step aims to remove all the phase disturbances from the L1c stack and set terrain phase at zero height (i.e., subtract DTM phase). Each polarization channel is processed independently. The SCS L1c stack provided as input contains a set of calibration and ground steering phase screens (SKP calibration screens and flattening phases screens described in [RD1]). Depending on *applyCalibrationScreen* configuration, the used screen is:

$\varphi = \varphi_{skp} + \varphi_{flattening}$ if *applyCalibrationScreen= "skp"*

$\varphi = \varphi_{flattening}$ if *applyCalibrationScreen= "geometry"*

The operation implemented in the calibration step of the L2 processor is simply the subtraction of the selected calibration phase screens from the input image stack phase. The operation can be expressed as:

$$SCS(r,a,n) = SCS(r,a,n)e^{+j\varphi(r,a,n)} \quad (3.2)$$

where $\varphi(r,a,n)$ is the phase screen accounting for all the disturbance terms and terrain topography relative to the baseline n for each pixel in azimuth a, slant-range r. In the case of the reference acquisition, no compensation is done (zero baseline). If the phase screens have a lower resolution than the SCSs then a preliminary interpolation step is needed. The operation can be expressed as:

$$\varphi(r,a,n) = f\left[\varphi(r,a,n)|_{(rg,\varphi,az,\varphi)}\right]\Big|_{(rg,az)} \quad (3.3)$$

where *f* is a bilinear interpolant a function. Other alternate interpolating function are detailed in [RD15].

3.4. Coherence estimation

3.4.1. Overview and rationale

The coherence estimation block aims to estimate the second order polarimetric-interferometric statistics of phase calibrated and ground steered (terrain at zero level) L1c stack and compensate non-volumetric decorrelation. In the following its implementation in the context of the INT Phase, i.e., by means of the three fully polarimetric images acquired in a repeat-pass mode with a spatial baseline between consecutive orbits is defined. This is applied also in the TOM Phase by choosing the same baselines of the INT Phase, see sec. 3.2. The flowchart of the algorithm is shown in the figure below.

The step is mandatory.

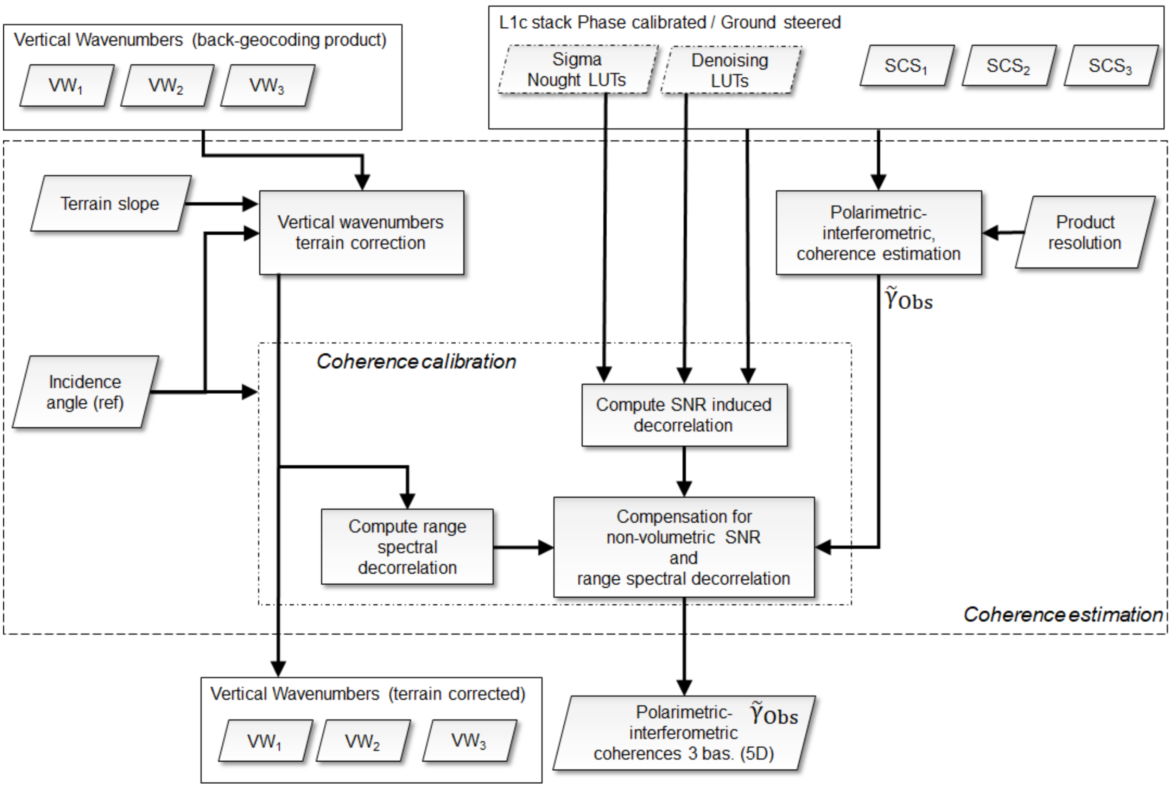

Fig.7 Coherence estimation algorithm (INT/TOM Phase).

3.4.2. Inputs

Symbol	Name	Origin	Size	Variability	Default	Description
SCS	L1c	*Calibration step*	M, each acquisition $[N_{rg} \times N_{az}]$	M=3 acquisitions with two CP and one XP	-	Phase calibrated and ground steered (terrain at zero level) L1c stack
-	spectralDecorrelationCompensationFlag	AUX_PP2_2A (AUX_FMT)	Boolean [scalar]	-	True	True (default value) if range spectral decorrelation compensation has to be performed, False otherwise
-	SNRDecorrelationCompensationFlag	AUX_PP2_2A (AUX_FMT)	Boolean [scalar]	-	True	True (default value) if SNR decorrelation compensatio

Symbol	Name	Origin	Size	Variability	Default	Description
						n has to be performed, False otherwise
pRes	ProductResolution	AUX_PP2_2A (AUX_FMT)	float value [scalar]	-	200.0	Value in [m] to be used as the resolution on ground grange map and also to perform the coherence averaging in radar coordinates
-	upsamplingFactor	AUX_PP2_2A (AUX_FMT)	int value [scalar]	-	2	upsampling factor, that modules the overall decimation in multilooking within coherence computation
σ_{LUT}^{noise}	denoising	L1c Stack ADS (L1_PFD)	M, each acquisition $[N_{rg,noise} \times N_{az,noise}]$	-	-	denoising LUT
σ_{LUT}^{0}	sigmaNought	L1c Stack ADS (L1_PFD)	M, each acquisition $[N_{rg,sigma} \times N_{az,sigma}]$	-	-	sigmaNought LUT
α	terrainSlope	L1c reference acquisition ADS (L1_PFD)	$[N_{rg,\alpha} \times N_{az,\alpha}]$	-	-	Terrain slope [rad]
θ_0	incidenceAngle	L1c reference acquisition ADS (L1_PFD)	$[N_{rg,\theta} \times N_{az,\theta}]$	-	-	L1c stack reference acquisition incidence angle [deg] (on inflated ellipsoid) annotation
k_z	wavenumber	L1c Stack ADS (L1_PFD)	M, each $[N_{rg,k} \times N_{az,k}]$ (zero	-	-	Vertical wavenumbers [rad/m] computed

Symbol	Name	Origin	Size	Variability	Default	Description
			for reference acquisition)			with respect to incidence on inflated ellipsoid
B_r	L1c range-bandwidth	L1c reference acquisition ADS (L1_PFD)	-	-	-	L1c range bandwidth [Hz]
B_a	L1c azimuth bandwidth	L1c reference acquisition ADS (L1_PFD)	-	-	-	L1c range bandwidth [Hz]
v_a	L1c velocity annotation	L1c reference acquisition ADS (L1_PFD)	-	-	-	Average azimuth velocity [m/s]
Δ_r	L1c range-sampling step	L1c reference acquisition ADS (L1_PFD)	-	-	-	L1c range sampling step [s]
Δ_a	L1c azimuth sampling step	L1c reference acquisition ADS (L1_PFD)	-	-	-	L1c azimuth sampling step [s]
	correctTerrainSlopesFlag	AUX_PP2_2A (AUX_FMT)	bool	-	True	True if terrain slope correction must been applied, False otherwise

3.4.3. Outputs

Symbol	Name	Destination	Size	Variability	Default	Description
$\tilde{\gamma}_{\mathrm{Obs}}$	-	*Forest height inversion step*	$[N_{pol} \times N_{pol} \times N_{bas} \times N_{rg,subs} \times N_{az,subs}]$	-	-	Polarimetric-interferometric coherence for three spatial baselines

Symbol	Name	Destination	Size	Variability	Default	Description
k_z	wavenumber	*Forest height inversion step*	M, each $[N_{rg,k} \times N_{az,k}]$ (zero for reference acquisition)	-	-	Terrain corrected vertical wavenumbers [rad/m] computed with respect to incidence on inflated ellipsoid

3.4.4. Algorithm mathematical background

3.4.4.1. Polarimetric-interferometric coherence estimation

The size of the spatial averaging window used to estimate the second order statistics depends on the final resolution of the products to be provided as an input. The output is a 5D array with dimensions: $[N_{pol} \times N_{pol} \times N_{bas} \times N_{rg,subs} \times N_{az,subs}]$ where N_{pol} is the number of polarizations, N_{bas} the number of unique spatial baselines, and $N_{rg,subs}$ and $N_{az,subs}$ are the numbers of range and azimuth samples after subsampling (half window size, well complying with the Nyquist-Shannon sampling theorem). For each (subsampled) range-azimuth position a $N_{pol} \times N_{pol}$ multi-polarimetric coherence matrix is returned for each unique spatial baseline, i.e., $n \neq m \wedge nm = mn$. Mathematically for each (subsampled) range-azimuth position (notation is simplified omitting range-azimuth indexes for the sake of clarity):

$$\tilde{\gamma}_{\text{Obs}}({k_z}^{nm}, \mathrm{w}^{pq}) = \frac{\sum_{r\in\Omega_r}\sum_{a\in\Omega_a} y_{p,n}(r,a)\cdot y^*_{q,m}(r,a)}{\sqrt{\sum_{r\in\Omega_r}\sum_{a\in\Omega_a} y_{p,n}(r,a)\cdot y^*_{p,n}(r,a)}\sqrt{\sum_{r\in\Omega_r}\sum_{a\in\Omega_a} y_{q,m}(r,a)\cdot y^*_{q,m}(r,a)}} \tag{3.4}$$

where w^{pq} denote the p-th and q-th polarimetric channels respectively; r and a denote the range and azimuth indices; Ω_r and Ω_a denote the neighborhood in the range and azimuth directions of the desired position; $y_{p,n}(r,a)$ denotes the complex pixel value in SCS polarimetric channel p for acquisition n; ${k_z}^{nm} = k_z(r,a,m) - k_z(r,a,n)$ is the nm interferometric pair vertical wavenumber depending on baseline; $*$ denotes conjugation . The averaging window size is computed as:

$$|\Omega_r| = \left\lceil \frac{pRes}{\rho_r} \sin\theta_m \, (\Delta_r B_r)^{-1} \right\rceil \tag{3.5}$$

$$|\Omega_a| = \left\lceil \frac{pRes}{\rho_a} (\Delta_a B_a)^{-1} \right\rceil$$

where $\rho_r = \frac{c}{2B_r}$ and $\rho_a = \frac{\mathrm{v}_a}{B_a}$ denote the L1c resolution computed from system bandwidth, Lightspeed *c*, average azimuth velocity v_a, *pRes* is the L2 resolution, $\theta_m = \frac{1}{N_r N_a}\sum_{r,a}\theta_0(r,a)$ is the average incidence angle across the swath, while the terms $(\Delta_i B_i)^{-1}, i = r, a$ represent the oversampling factor.. SCS invalid pixels will not be used during processing. The presence of an invalid SCS pixel causes the generation of an invalid coherence sample.

3.4.4.2. Vertical wavenumbers terrain correction

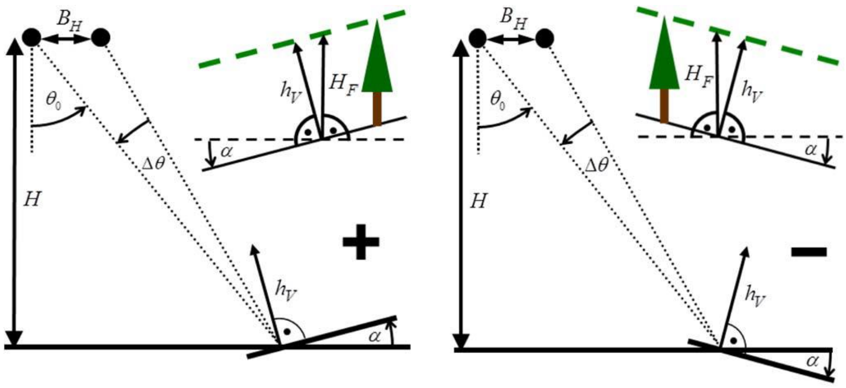

Fig.8 Acquisition geometry with terrain slope α [RD6]. (a) Positive terrain slope. (b) Negative terrain slope. B_H is the horizontal baseline, H is the flight height, θ_0 the incidence angle between radar beam and the local normal to the inflated ellipsoid (tangent plane to ellipsoid represented by horizontal line), Δθ the angle difference induced by the baseline, h_V the height of the volume and H_F the height of the forest.

Terrain slopes in range direction (indicated by α in Fig.8) modify locally the incidence angle θ_0 of reference acquisition to $\theta=\theta_0-\alpha$ and as a consequence the vertical wavenumbers must be corrected as:

$$k_z(r,a,n) = k_z(r,a,n)\frac{\sin[\theta_0(r,a)]}{\sin[\theta_0(r,a)-\alpha(r,a)]} \tag{3.6}$$

where r and a denote the range and azimuth indices for acquisition n. A preliminary interpolation step is needed to bring wavenumbers, slope, angle onto the same coherence grid, in similar fashion as for the calibration screens (Section 3.3.4). The correction above is performed only when correctTerrainSlopesFlag is set to true.

3.4.4.3. Coherence calibration

Non-volumetric SNR $\tilde{\gamma}_{\mathrm{SNR}}$ and range spectral decorrelation $\tilde{\gamma}_{\mathrm{Rg}}$ are compensated (<u>each subsampled range-azimuth position is processed separately</u>; notation is simplified omitting range-azimuth indexes for the sake of clarity)

$$\tilde{\gamma}_{\mathrm{Obs}}({k_z}^{nm},\mathrm{w}^{pq}) = \frac{\tilde{\gamma}_{\mathrm{Obs}}({k_z}^{nm},\mathrm{w}^{pq})}{\tilde{\gamma}_{\mathrm{Rg}}({k_z}^{nm})\tilde{\gamma}_{\mathrm{SNR}}({k_z}^{nm},\mathrm{w}^{pq})} \tag{3.7}$$

where

$$\tilde{\gamma}_{\mathrm{Rg}}({k_z}^{nm}) = 1-\frac{\rho_r}{2\pi/{k_z}^{nm}} \tag{3.8}$$

where ρ_r is the bandwidth limited range resolution and ${k_z}^{nm}$ is the nm interferometric pair vertical wavenumber depending on baseline. The SNR induced decorrelation $\tilde{\gamma}_{\mathrm{SNR}}({k_z}^{nm},\mathrm{w}^{pq})$ in the corresponding interferogram acquired by two different polarimetric channels p and q is obtained as [RD9]

$$\tilde{\gamma}_{\mathrm{SNR}}({k_z}^{nm}, \mathrm{w}^{pq}) = \frac{1}{\sqrt{\left[1+\frac{1}{\mathrm{SNR}(p,n)}\right]\left[1+\frac{1}{\mathrm{SNR}(q,m)}\right]}} \tag{3.9}$$

where

$$\mathrm{SNR}(p,n) = \frac{\beta^0(p,n)\sigma^0_{LUT}(p,n) - \sigma^{noise}_{LUT}(p,n)}{\sigma^{noise}_{LUT}(p,n)} \tag{3.10}$$

where $\beta^0(p,n) = \frac{1}{N_{\Omega_r}N_{\Omega_a}}\sum_{r\in\Omega_r}\sum_{a\in\Omega_a} y_{p,n}(r,a)\cdot y^*_{p,n}(r,a)$ is the backscattering coefficient (see sec. 3.4.4.1 for notation), $\sigma^0_{LUT}(p,n)$ is the sigma Nought conversion factor from two-dimensional LUT for acquisition n and $\sigma^{noise}_{LUT}(p,n)$ is the noise equivalent sigma zero from two-dimensional LUT for acquisition n [AD2]. Multi-look Ω_r and Ω_a applied to obtain SNR decorrelation must be consistent with that of polarimetric-interferometric coherence estimation. Being sigma and noise defined over a coarsely sub-sampled grid with respect to the SAR image, a bilinear interpolation of the LUT is required before its application on the data. The operation can be expressed as:

$$\begin{aligned}\sigma^{noise}_{LUT}(p,n) &= f\left[\sigma^{noise}_{LUT}(p,n)\big|_{(rg,noise,az,noise)}\right]\Big|_{(rg,subs,az,subs)}\\ \sigma^0_{LUT}(p,n) &= f\left[\sigma^0_{LUT}(p,n)\big|_{(rg,sigma,az,sigma)}\right]\Big|_{(rg,subs,az,subs)}\end{aligned} \tag{3.11}$$

where *f* is a bilinear interpolant a function.

3.4.5. Notes on implementation

It should be noted that, as implied by the equations above, multilooking is implicitly performed while computing coherence. The ratio of subsampling of the final coherence image (i.e., the step where full matrix is sampled) is ruled by the “upsamplingFactor” parameter: when the assumed value is 1, full subsampling is applied ($N_{rg|az,subs} = N_{rg|az} / N_{\Omega r|az}$),while when its value is higher, the final output coherence will be bigger ($N_{rg|az,subs} = N_{rg|az} / N_{\Omega r|az}$ * upsamplingFactor).

3.5. Forest height inversion

3.5.1. Overview and rationale

The forest height inversion algorithm aims to generate maps of forest upper canopy height (H100 Standard) by means of a model-based inversion based on the so-called Random Volume over Ground (RVoG) model accounting for a polarization invariant vertical volume reflectivity function, a 3D polarimetric ground scattering component and a scalar temporal decorrelation of the volume layer. The implementation here described relies on the use of a modeled or tomographically derived volume-only reflectivity profile normalized to unit height, following the approach [RD10]. The default forest height inversion method is dual-baseline, the alternative method is single-baseline, the flowchart of the algorithm is shown in figure below. **The following processing applies to each subsampled range-azimuth position. The notation is simplified omitting range-azimuth indexes for the sake of clarity.**

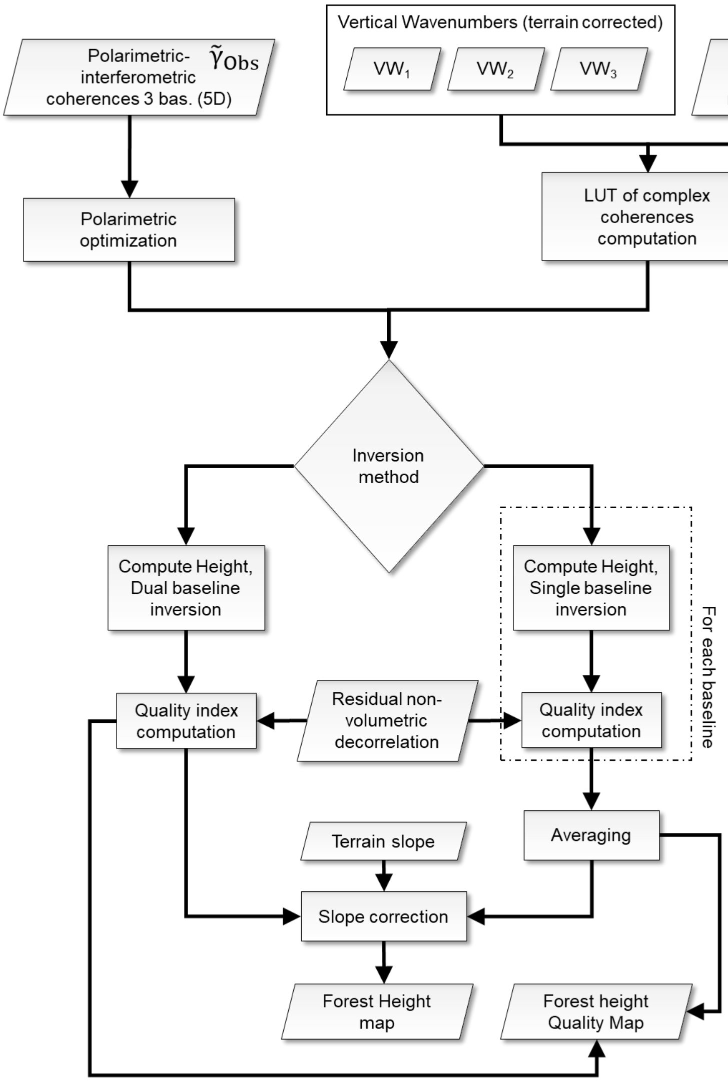

Fig.9 Forest height inversion.

The step is mandatory.

3.5.2. Inputs

Symbol	Name	Origin	Size	Variability	Default	Description
$\tilde{\gamma}_{\mathrm{Obs}}$	-	*Coherence estimation step*	$[N_{pol} \times N_{pol} \times N_{bas} \times N_{rg,subs} \times N_{az,subs}]$	-	-	Polarimetric-interferometric coherence for three spatial baselines
k_z	wavenumber	*Coherence estimation step*	M, each $[N_{rg,k} \times N_{az,k}]$ (zero for reference acquisition)	-	-	Terrain corrected vertical wavenumbers [rad/m] computed with respect to incidence on inflated ellipsoid
$\tilde{\gamma}_{\mathrm{deco}}$	residualDecorrelation	AUX_PP2_2A (AUX_FMT)	float value [scalar]	Global single value for all pixels ranging 0.0-1.0	0.97	Residual non-volumetric decorrelation to be used in error model computation
$\mathrm{P_V}$	verticalReflectivityDefaultProfile	AUX_PP2_2A (AUX_FMT)	N_{h}	deterministic and fixed for all the globe	-	Modeled tomographic volume-only reflectivity profile normalized to unit height
-	verticalReflectivityOption	AUX_PP2_2A (AUX_FMT)	string	-	“default profile”	Specify which vertical reflectivity profile to use: default modelled profile or tomographic profile (out of BPS scope)
-	modelInversion	AUX_PP2_2A (AUX_FMT)	string	-	“dual baseline”	Model inversion algorithm to be used among single

Symbol	Name	Origin	Size	Variability	Default	Description
						or dual baseline
α	terrainSlope	L1c reference acquisition ADS (L1_PFD)	$[N_{rg,\alpha} \times N_{az,\alpha}]$	-	-	Terrain slope [deg]
h	normalisedHeightEstimationRange	AUX_PP2_2A (AUX_FMT)	2 float value minMax	-	[0.0, 1.0]	Range of normalized height values where the canopy height estimation process has to be performed
k_{h}	normalisedWavenumberEstimationRange	AUX_PP2_2A (AUX_FMT)	32 float, 1 int minMax Num= $N_{k_{\mathrm{h}}}$	-	[0.0, 2π, 125.0]	Range of normalized wavenumbers values where the canopy height estimation process has to be performed: Num to set sensitivity of 1 [m] for smaller k_z value of 0.05 [1/m]
m	groundToVolumeRatioRange	AUX_PP2_2A (AUX_FMT)	2 float , 1 int minMax Num= N_{m}	-	[-20.0, 20.0, 30]	Range of ground to volume ratio values to be used as valid ones [dB]
γ_{TempV}	temporalDecorrelationEstimationRange	AUX_PP2_2A (AUX_FMT)	2 float, 1 int minMax Num= N_{TempV}	-	[0.3, 1.0, 30]	Range of temporal decorrelation values to be used as valid ones
$\mathrm{R}_{\mathrm{TempGV}}$	temporalDecorrelationGroundToVolumeRatio	AUX_PP2_2A (AUX_FMT)	float value [scalar]	0.0, 1.0	1.0	Ratio of temporal decorrelation between

Symbol	Name	Origin	Size	Variability	Default	Description
						ground and volume (0.0 means no temporal decorrelation for ground, while 1.0 means ground and volume are equally impacted by temporal decorrelation)
-	uncertaintyValidvaluesLimits	AUX_PP2_2A (AUX_FMT)	2 float value	-	[0.0%, 100.0%]	Uncertainty valid values limits: FH estimates are put to no data when corresponding uncertainty values are out of these limits
-	verticalWavenumberValidvaluesLimits	AUX_PP2_2A (AUX_FMT)	2 float value	-	[0.01, 0.19]	Vertical wavenumber valid values limits in [1/m]: FH estimates are put to no data when corresponding wavenumber values are out of these limits
-	lowerHeightLimit	AUX_PP2_2A (AUX_FMT)	1 float value	-	0.0	FH estimates lower this limit [m] are discarded and set to no data value
	correctTerrainSlopesFlag	AUX_PP2_2A (AUX_FMT)	bool	-	True	True if terrain slope correction

Symbol	Name	Origin	Size	Variability	Default	Description
						must been applied, False otherwise

The default operation mode is modelInversion="dual baseline" with full INT stack [RD7]. To operate with a single pair configuration must be set to "single baseline". In case of only two images available, the modelInversion is automatically set to "single baseline".

A default constant modeled profile is provided as a configuration [RD7]. It can be substituted with profile derived from TOM data (out of BPS scope).
The default modeled vertical reflectivity in configuration is provided by DLR and represents Gaussian fit of real average tomographic reflectivity over AfriSAR Lope test site [RD5]. The fit is done on volume only reflectivity (excluding terrain) and the function is normalized by the peak value, so as to be scaled from 0 to 1. The resulting vector has size $N_{\mathrm{h}} = 70$ samples, chosen so as to be correspondent to 1m sampling over the non-normalized reflectivity. The vertical sampling choice is conservative and allows the model to better account for terrain Dirac delta. This function represents a realistic forest reflectivity shape and corresponds to the choice of fixing a shape/extinction parameter [RD9], it is used as a default choice globally (the algorithm scales in any case the reflectivity function within the normalized height range, which is then mapped to real height range through the wavenumber within the algorithm). The default modeled vertical reflectivity is shown in Fig.10.

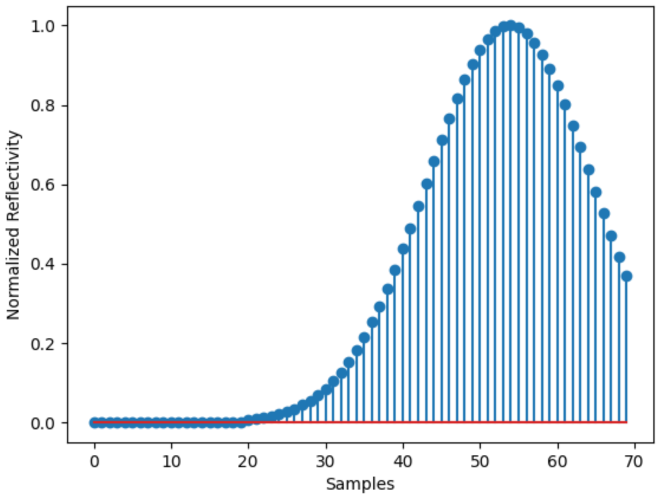

Fig.10 Modeled vertical reflectivity.

The TOM-derived reflectivity is out of BPS scope. The post-launch activities will be devoted to analysing TOM acquisitions so as to derive a vertical reflectivity basis representative of the forest types on global scale, through algebraic decomposition such as in [RD10]. The same peak normalization can be applied to TOM reflectivity, the vertical sampling is in this case oriented to 5m from project requirements [RD12]. Interpolation to 1m can be done subsequently.

3.5.3. Outputs

Symbol	Name	Destination	Size	Variability	Default	Description
$\mathrm{H_F}$	forest height	*Geocoding step*	$[N_{rg,subs} \times N_{az,subs}]$	-	-	Forest height map
$\mathrm{h_b}$	forest height quality	*Geocoding step*	$[N_{rg,subs} \times N_{az,subs}]$	-	-	Quality index indicating the inversion performance

3.5.4. Algorithm mathematical background

3.5.4.1.1. Polarimetric optimization

The availability of fully-polarimetric data allows the implementation of coherence optimization as a pre-processing step. The aim of this step is to exploit the polarisation diversity to improve the inversion performance. This optimization may be performed for each spatial baseline individually by means of computing the centre of mass (Trace coherence) of polarimetric coherence region, which is, in terms of the Frobenius norm, the best approximation, of the coherence region by a single point [RD11]. Mathematically:

$$\tilde{\gamma}_c({k_z}^{nm}) = \left. \frac{trace(\tilde{\gamma}_{\mathrm{Obs}}({k_z}^{nm}, \mathrm{w}^{pq}))}{3} \right|_{\mathrm{w}^{pq}} \tag{3.12}$$

where $\tilde{\gamma}_{\mathrm{Obs}}({k_z}^{nm}, \mathrm{w}^{pq})$ denote calibrated coherence as in section 3.4.4.3 and trace is computed by the polarimetric axes w^{pq}. Result has dimension $[N_{bas}]$ at each subsampled range-azimuth position.

3.5.4.1.2. LUT of complex coherences computation

The inversion relies on the generation of a look-up table containing forward modelled coherence for each value of normalized vertical wavenumber $k_{\mathrm{h}} = k_z z$, scalar temporal decorrelation γ_{TempV} (ancillary parameter) and ground-to-volume ratio m (ancillary parameter converted between decibels and a linear scale). Mathematically:

$$\tilde{\gamma}_{\mathrm{VolT}}(k_{\mathrm{h}}, \gamma_{\mathrm{TempV}}, \mathrm{m}) = \frac{\gamma_{\mathrm{TempV}}\, \tilde{\gamma}_{\mathrm{V0}}(k_{\mathrm{h}}) + \mathrm{m} - \mathrm{R}_{\mathrm{TempGV}}(1 - \gamma_{\mathrm{TempV}})\mathrm{m}}{1 + \mathrm{m}} \tag{3.13}$$

where

$$\tilde{\gamma}_{V0}(k_h) = \frac{\sum_{N_h} P_V(h)\exp(ik_h\,h)}{\sum_{N_h} P_V(h)} \tag{3.14}$$

where from default configuration $h \in [0,1]$, $k_h \in [0,2\pi]$, $m \in [0.01,100]$, $\gamma_{TempV} \in [0.3,1]$, $P_V(h)$ is the volume-only tomographic reflectivity profile normalised to unit height, N_h the number of height samples (ruling also h vectors size). The parameter intervals are sampled to generate the LUT with dimensions: $[N_{k_h} \times N_{TempV} \times N_m]$. For single baseline case the LUT assumes $m = 0$, $\tilde{\gamma}_{VolT} = 1$, the LUT has dimension: $[N_{k_h}]$.

3.5.4.1.3. Dual-baseline inversion

The default forest height inversion method is dual-baseline [RD6],[RD9], where the two baselines are chosen from the set $\{{k_z}^{nm} | n \neq m \wedge nm = mn\}$ and by default equal to ${k_z}^{max} = max\{{k_z}^{nm} | n \neq m \wedge nm = mn\}$ and ${k_z}^{min} = min\{{k_z}^{nm} | n \neq m \wedge nm = mn\}$. The cost function minimized is:

$$min_{k_h,{\gamma_{TempV}}^{min},{\gamma_{TempV}}^{max},m}\left\{\left\|\tilde{\gamma}_{VolT}\left(k_h,{\gamma_{TempV}}^{max},m\right) - \tilde{\gamma}_c({k_z}^{max})\right\|_2^2 + \left\|\tilde{\gamma}_{VolT}\left(k_h,{\gamma_{TempV}}^{min},m\right) - \tilde{\gamma}_c({k_z}^{min})\right\|_2^2\right\} \tag{3.15}$$

where $\tilde{\gamma}_c$ denote optimized coherence as in section 3.5.4.1.1. and $\tilde{\gamma}_{VolT}$ denote forward modelled coherence as in section 3.5.4.1.2. The model is inverted by fitting the same $\tilde{\gamma}_{VolT}$ LUT to computed coherences for the min and max baselines and a value of γ_{TempV} is estimated for the max and min baselines ${\gamma_{TempV}}^{max}$, ${\gamma_{TempV}}^{min}$. The two cost functions are computed to the same parameter and height sampling reference e.g., that of ${k_z}^{max}$. It means that k_h axis of $\tilde{\gamma}_{VolT}$ has a range of $k_h \in [0,2\pi]$ for ${k_z}^{max}$ and a range of $k_h \in [0,2\pi]\frac{{k_z}^{min}}{{k_z}^{max}}$ for ${k_z}^{min}$. Volume height is finally calculated as:

$$h_V = \frac{\widetilde{k_h}}{|{k_z}^{max}|} \tag{3.16}$$

where $\widetilde{k_h}$ results from cost function minimization.

3.5.4.1.4. Notes on efficient implementation

Relation 3.15 implies the minimization of a compound cost function (sum of two real-valued semi-positive terms) in a 4-dimensional space: $k_h, {\gamma_{TempV}}^{min}, {\gamma_{TempV}}^{max}, m$. The chosen inversion strategy is based on a brute-force approach (note that the terms that depend on the parameters to be minimized are precomputed and available in a LUT, relation 3.13).
As the minimum of any sum of semi-positive real functions is equivalent to the sum of the minima, the minimization problem can be re-expressed as a separable two-stage linear search, each one in a 3-dimensional space: k_h, γ_{TempV}, m.

Nonetheless, the original formulation requires $\left[N_{k_\mathrm{h}} \times N_{\mathrm{TempV}} \times N_{\mathrm{TempV}} \times N_\mathrm{m}\right]$ evaluations of the cost function, while the separable one requires only $\left[2 \times N_{k_\mathrm{h}} \times N_\mathrm{m}\right]$ minimizations of 1D arrays of size N_{TempV}, followed by a minimization over a 2D array of size $\left[N_{k_\mathrm{h}} \times N_\mathrm{m}\right]$.

As an example, with a LUT of size $\left[N_{k_\mathrm{h}} = 125,\ N_{\mathrm{TempV}} = 20,\ N_\mathrm{m} = 21\right]$, the original formulation requires 1050000 evaluations of the cost function, while the separable one is roughly equivalent to a linear search over an array of 107625 elements (1/10th of the original problem size).

3.5.4.1.5. Single-baseline inversion

The alternative forest height inversion method is single-baseline [RD6][RD9], inversion is computed for each baseline. For each baseline cost function minimized is:

$$min_{k_\mathrm{h}} \left| t\left[\tilde{\gamma}_{\mathrm{VolT}}\left(k_\mathrm{h}, \gamma_{\mathrm{TempV}} = 1, \mathrm{m} = 0\right)\right] - t[\tilde{\gamma}_c({k_z}^{nm})] \right| \tag{3.17}$$

$$t[\gamma] = \tan^{-1}\left\{\frac{1 - Real[\gamma]}{Imag[\gamma]}\right\}$$

where $\tilde{\gamma}_c$ denote optimized coherence as in section 3.5.4.1.1 and $\tilde{\gamma}_{\mathrm{VolT}}$ denote forward modelled coherence as in section 3.5.4.1.2. Volume height is calculated as:

$$\mathrm{h_V} = \frac{\widetilde{k_\mathrm{h}}}{|{k_z}^{nm}|} \tag{3.18}$$

where $\widetilde{k_\mathrm{h}}$ results from cost function minimization.

Estimates are finally combined by performing an average, using quality information h_b^i computed as in section 3.5.4.1.6:

$$\mathrm{h_V} = \frac{\sum_i \frac{1}{\varepsilon + h_b^i} {\mathrm{h_V}}^i}{\sum_i \frac{1}{\varepsilon + h_b^i}} \tag{3.19}$$

$$\mathrm{h}_b = \frac{\sum_i \frac{1}{\varepsilon + h_b^i} h_b^i}{\sum_i \frac{1}{\varepsilon + h_b^i}}$$

where $\varepsilon = 0.01$ is an adjustment factor.

3.5.4.1.6. Quality index computation

The theoretical forward modelled volume-only coherence after applying a residual non-volumetric decorrelation is calculated for normalized vertical wavenumber $\widetilde{k_\mathrm{h}}$ resulting from estimation described in sec. 3.5.4.1.3 for dual-baseline and in sec. 3.5.4.1.5 for each single-baseline, as

$$\tilde{\gamma}_{\mathrm{VolTdeco}} = \tilde{\gamma}_{\mathrm{VolT}}\left(\widetilde{k_\mathrm{h}}, \gamma_{\mathrm{TempV}} = 1, \mathrm{m} = 0\right)\tilde{\gamma}_{\mathrm{deco}} \tag{3.20}$$

where $\tilde{\gamma}_{\mathrm{deco}} \in (0,1)$ is a configuration parameter and $\tilde{\gamma}_{\mathrm{VolT}}$ denotes forward modelled coherence as in section 3.5.4.1.2. $\tilde{\gamma}_{\mathrm{VolTdeco}}$ is inverted following the single-baseline approach in sec. 3.5.4.1.5 and ${k_\mathrm{h}}^\mathrm{b}$ results from cost function minimization:

$$min_{k_h} \left| t\left[\tilde{\gamma}_{\mathrm{VolT}}\left(k_h, \gamma_{\mathrm{TempV}} = 1, \mathrm{m} = 0\right)\right] - t\left[\tilde{\gamma}_{\mathrm{VolTdeco}}\right] \right| \tag{3.21}$$

$$t[\gamma] = \tan^{-1}\left\{\frac{1 - Real[\gamma]}{Imag[\gamma]}\right\}$$

Percentage bias as a quality index is finally calculated as:

$$\mathrm{h_b} = \left|\frac{k_h{}^{\mathrm{b}} - \widetilde{k_h}}{\widetilde{k_h}}\right| \cdot 100 \tag{3.22}$$

This quality index can be estimated for each forest height inversion as in section 3.3.3.1.4 or section 3.5.4.1.3.

3.5.4.1.7. Correction of terrain slope

The resulting volume heights h_V are transferred into a forest height H_F as in Fig.8. Mathematically, for sloped terrain it results (each subsampled range-azimuth position is processed separately):

$$\mathrm{H_F} = \frac{\mathrm{h_V}}{\cos\alpha} \tag{3.23}$$

where α denote terrain slope.This correction is performed only when correctTerrainSlopesFlag is set to true.

3.5.4.1.8. Valid values thresholding

The resulting forest height H_F and quality estimates out of uncertaintyValidvaluesLimits, verticalWavenumberValidvaluesLimits, lowerHeightLimit are discarded and set to no data value. Note: the FNF is not updated instead.

3.6. Geocoding

3.6.1. Overview and rationale

The purpose of this step is to project the processed data onto a geographic map, accounting for the different forest points location with respect to reference DEM.

NOTE: It should be noted that the use of the BIOMASS DTM [RD3] is to be preferred to other DEM since it represents the true terrain level at P-band, necessary for correct geocoding.

NOTE: this functionality is used by all three AGB, FD, FH processors with different I/O. mathematical formulation is described highlighting the mapping of the different processors I/O to geocoding formulas in each processor document. The functionality relies on L1c ADS [RD1] and not on the L1 geocoding tool [RD2].

The step is mandatory.

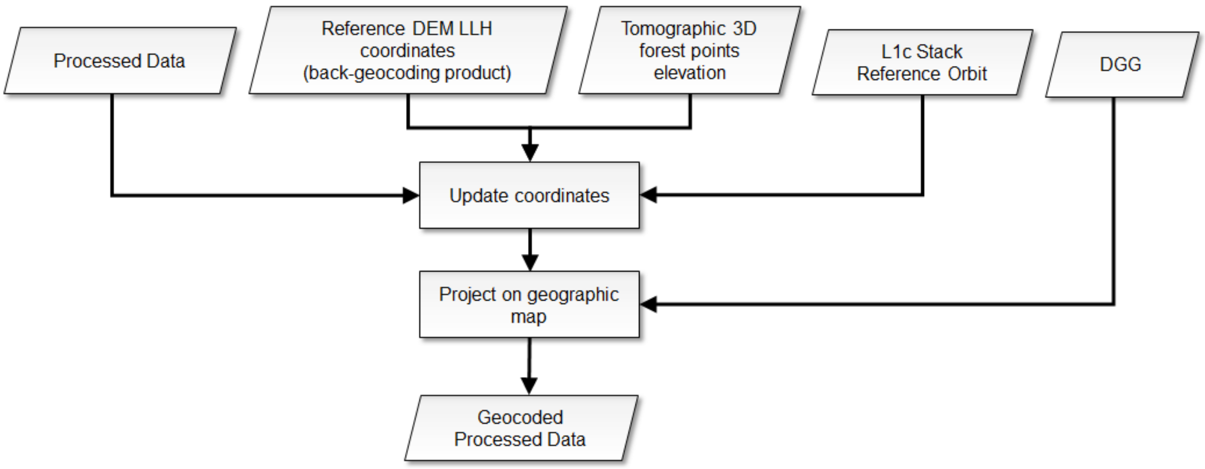

Fig.11 Geocoding.

3.6.2. Inputs

Symbol	Name	Origin	Size	Variability	Default	Description
$\mathrm{H_F}, \mathrm{h_b} \rightarrow Rd$	-	*Forest height inversion step*	2x $[N_{rg,subs} \times N_{az,subs}]$	-	-	Processed data, in this case forest height map and quality index of current stack
(lat, lon, z_{P_0})	latitude longitude height	L1c reference acquisition ADS (L1_PFD)	3x $[N_{rg,\mathrm{llh}} \times N_{az,\mathrm{llh}}]$	-	-	Reference DEM latitude-longitude-height coordinates
$\mathrm{H_F} \rightarrow \delta z_{tomo}$	-	*Forest height inversion step*	$[N_{rg,subs} \times N_{az,subs}]$	-	-	Tomographic 3D forest points elevation [m], in this case forest height map
DGG	*DGG*	Internal lookup table	-	-	-	DGG sampling
$\hat{\imath}_{az}$	Orbit ADS	L1c reference acquisition ADS (L1_PFD)	-	-	-	L1c stack reference acquisition orbit annotation

3.6.3. Outputs

Symbol	Name	Destination	Size	Variability	Default	Description
Rd	-	*FNF annotation step*	2x $[N_{lat} \times N_{lon}]$	-	-	forest height map and quality index of current stack projected onto a geographic map

3.6.4. Algorithm mathematical background

3.6.4.1.1. Update reference DEM coordinates

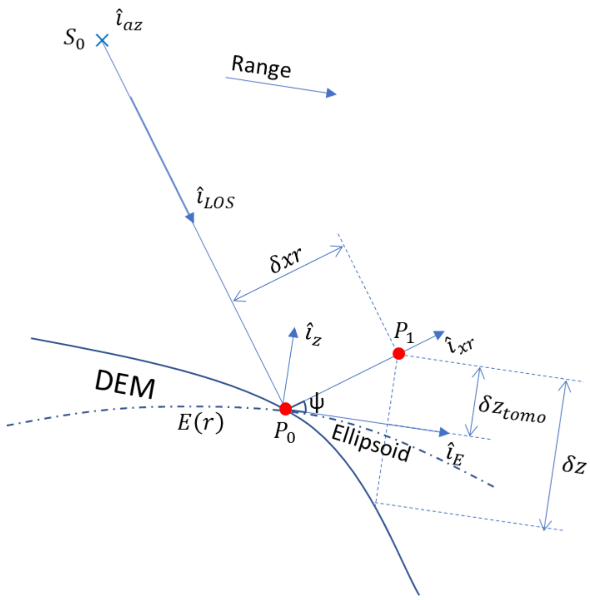

Fig.12 Determining the elevation of one forest point. The picture represents a lateral section for one sensor azimuth position. Details of the represented quantities are given in the text description.

This step aims to account for the different forest points location with respect to reference DEM. A preliminary interpolation step is needed to bring DEM latitude-longitude-height onto the same forest height range-azimuth grid, in similar fashion as for the calibration screens (Section 3.3.4). Determining the elevation of one forest point is shown in Fig.12:

- (lat, lon, z_{P_0}) is the reference DEM for the point $\boldsymbol{P}_0$, which can be converted to Cartesian coordinates $(X_{P_0}, Y_{P_0}, Z_{P_0})$
- z is normal direction to ellipsoid reported to DEM at point $\boldsymbol{P}_0$, i.e., given the tangent plane to ellipsoid a X + b Y + c Z + d = 0 then $\hat{\imath}_z = [a, b, c\,]$
- $\hat{\imath}_{az}$ is the azimuth sensor direction, determined from reference orbit annotation
- $\hat{\imath}_{LOS} = \frac{\boldsymbol{P}_0 - \boldsymbol{S}_0}{|\boldsymbol{P}_0 - \boldsymbol{S}_0|}$ is line of sight vector, $\boldsymbol{S}_0$ is the sensor position for the considered azimuth
- $\hat{\imath}_{xr} = \hat{\imath}_{az} \times \hat{\imath}_{LOS}$ is the cross range vector
- the ellipsoid direction at reference DEM is $\hat{\imath}_E \cdot \hat{\imath}_z = 0$, i.e., $\hat{\imath}_E = \frac{d[\boldsymbol{E}(r)]}{dr}$ and $\boldsymbol{E}(r) = [X_E(r), Y_E(r), Z_E(r)]$ are ellipsoid coordinates as a function of range
- δz_{tomo} is one tomographic forest point elevation, in this case the point forest height
- δz is the elevation of point P1 versus DEM (with respect to WGS84 geodetic system). Note that while this is represented for completeness in Fig.12, it is not explicitly needed to compute P1 [x,y,z] position in the following eq 3.25.

Then

$$\delta xr = \frac{\delta z_{tomo}}{|\hat{\imath}_{xr} \times \hat{\imath}_E|} = \frac{\delta z_{tomo}}{sin(\psi)} \quad (3.24)$$

The geographic position of the forest point is:

$$\boldsymbol{P}_1 = \boldsymbol{P}_0 + \hat{\imath}_{xr} \cdot \delta xr \quad (3.25)$$

3.6.4.1.2. Projection onto a geographic map

Once the updated coordinates of the points are computed, interpolation of each raster layer to regular map coordinates projects the processed data onto a geographic map. In this case the information layers forest height and quality $Rd = \mathrm{H_F}, \mathrm{h_b}$ are both geocoded using the effective forest height represented (for each pixel) by $\delta z_{tomo} = \mathrm{H_F}$. Geocoding is done in a way that the products are sampled the same way onto the DGG sampling [RD8]. The operation can be expressed as:

$$Rd(lat, lon, z) \ = \ f\left[Rd(lat, lon, z)|_{\boldsymbol{P}_1}\right]\Big|_{DGG} \quad (3.26)$$

where *f* is a bilinear interpolant a function, *Rd* is each raster layer to be interpolated.

3.7. FNF annotation

3.7.1. Overview and rationale

The purpose of this step is to annotate the FNF in the L2a product.

The step is mandatory.

3.7.2. Inputs

Symbol	Name	Origin	Size	Variability	Default	Description
FNF	FNF	Internal resource (IODD)	$[N_{lat,FNF} \times N_{lon,FNF}]$	Yearly	-	A global forest-non-forest mask given as input
fMIT	forestMaskInterpolationThreshold	AUX_PP2_2A (AUX_FMT)	float value [scalar]	0.0-1.0	0.5	Threshold to fix rounding of pixels with decimal values originated from binary FNF interpolation onto L2a grid
Rd	-	*Geocoding step*	2x $[N_{lat} \times N_{lon}]$	-	-	forest height map and quality index of current

Symbol	Name	Origin	Size	Variability	Default	Description
						stack projected onto a geographic map

3.7.3. Outputs

Symbol	Name	Destination	Size	Variability	Default	Description
Rd	-	FH L2a product of current cycle (FH_PFD)	2x $[N_{lat} \times N_{lon}]$	-	-	forest height map and quality index of current stack projected onto a geographic map
FNF	FNF	FH L2a product of current cycle (FH_PFD)	$[N_{lat} \times N_{lon}]$	-	-	Annotated forest-non-forest mask

3.7.4. Algorithm mathematical background

The operation can be expressed as:

$$FNF(lat, lon) = f[FNF(lat, lon)|_{FNF}]|_{Rd} \tag{3.27}$$

where *f* is a bilinear interpolant a function. Since interpolation generates border effects a threshold *fMIT* to fix rounding of pixels with decimal values is applied:

$$FNF = FNF > fMIT \tag{3.28}$$

4. Forest height aggregation

The overall scheme of the L2b processing is reported in figure below.
The key step is fusion of L2a estimates at map level. These steps are described in detail in the following subsections.

4.1. L2a FH fusion

4.1.1. Algorithm overview and rationale

The forest height and quality maps allow the combination of different acquisitions in a simple and efficient pixelwise way. L2a products falling onto the same L2b tile within a global cycle are retrieved through geospatial query of information (tile IDs and time tags) in the Main Product Header of the product.

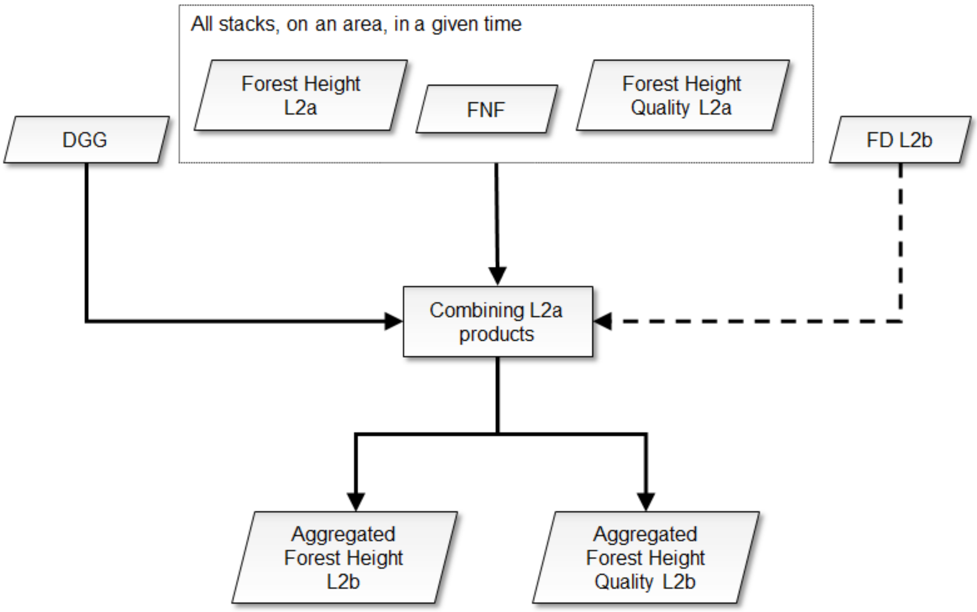

Fig.13 Complete flow-chart of the L2b processing.

The step is mandatory.

4.1.2. Inputs

Symbol	Name	Origin	Size	Variability	Default	Description
FNF^i	FNF	FH L2a products in a DGG tile in a global cycle (FH_PFD)	$[N_{lat} \times N_{lon}]^i$	-	-	Annotated forest-non-forest mask
H_F^i	forest height	FH L2a products in a DGG tile in a global cycle (FH_PFD)	$[N_{lat} \times N_{lon}]^i$	-	-	Forest height map
h_b^i	forest height quality	FH L2a products in a DGG tile in a global cycle (FH_PFD)	$[N_{lat} \times N_{lon}]^i$	-	-	Quality index indicating the inversion performance
CFM	CFM	FD L2b product in a DGG tile in a global cycle (FD_PFD)	$[N_{lat,L2b} \times N_{lon,L2b}]$	optional	not provided	Computed Forest Mask
-	forestMaskingFlag	AUX_PP2_FH (AUX_FMT)	bool	-	True	True if forest/non-forest map masking should be performed
DGG	DGG	Internal lookup table	-	-	-	DGG tile
BB^i	Footprint	L2a main product header (FH_PFD)	lat-lon vertices (4 couples)	-	-	The extent of the L2a input data in geographical coordinates
β_A	rollOffFactorAzimuth	AUX_PP2_FH (AUX_FMT)	float value [scalar]	0.0-1.0	0.1	Feathering roll-off factor
β_R	rollOffFactorRange	AUX_PP2_FH (AUX_FMT)	float value [scalar]	0.0-1.0	0.1	Feathering roll-off factor
mDGG	minimumL2aCoverage	AUX_PP2_FH (AUX_FMT)	float value [scalar]	0.0-100.0	10.0	The minimum [%] tile coverage that triggers the computations

4.1.3. Outputs

Symbol	Name	Destination	Size	Variability	Default	Description
H_F	forest height	FH L2b product	$[N_{lat,L2b} \times N_{lon,L2b}]$	-	-	forest height aggregated
h_b	forest height quality	FH L2b product	$[N_{lat,L2b} \times N_{lon,L2b}]$	-	-	forest height quality aggregated
HM	heat map	FH L2b product	$[N_{lat,L2b} \times N_{lon,L2b}]$	-	-	heat map

4.1.4. Algorithm mathematical background

As a first step, the minimum required coverage over L2b DGG tile *j* is checked to proceed with computations:

$$TR = \left(100 * \frac{A(\bigcup_i BB^i\big|_{DGG} \cap TT^j\big|_{DGG})}{A(TT^j|_{DGG})} > mDGG\right) \tag{4.1}$$

where BB^i are the L2a bounding boxes, TT^j is the footprint of the current L2b DGG tile and *A* operator computes the area of the corresponding polygon.

4.1.4.1. Feathering weights

Each L2a forest height map is weighted on its border (as defined by its footprint BB^i) by applying raised cosine weights and accounting for transitions between swaths [RD14]. Thus, the two feathering weights $w_{\mathrm{a}}^i(d) w_{\mathrm{r}}^i(d)$ are computed in the swath tilted domain, as defined by the footprint BB^i:

$$w_{a,r}^i(d) = \begin{cases} 1 & |d| \le \frac{1-\beta}{s_{\mathrm{w}}} \\ \frac{1}{2}\left[1 + \cos\left(\frac{\pi s_{\mathrm{w}}}{2\beta}\left[|d| - \frac{1-\beta}{s_{\mathrm{w}}}\right]\right)\right] & \frac{1-\beta}{s_{\mathrm{w}}} < |d| \le \frac{1+\beta}{s_{\mathrm{w}}} \\ 0 & otherwise \end{cases} \tag{4.2}$$

where $s_{\mathrm{w}} = s_{w,A}, s_{w,R}$ is swath width along azimuth or range direction (computed from swath footprint BB^i), d is distance from swath border (computed in the tilted domain) and $\beta = \beta_A, \beta_R$ is the roll-off factor.

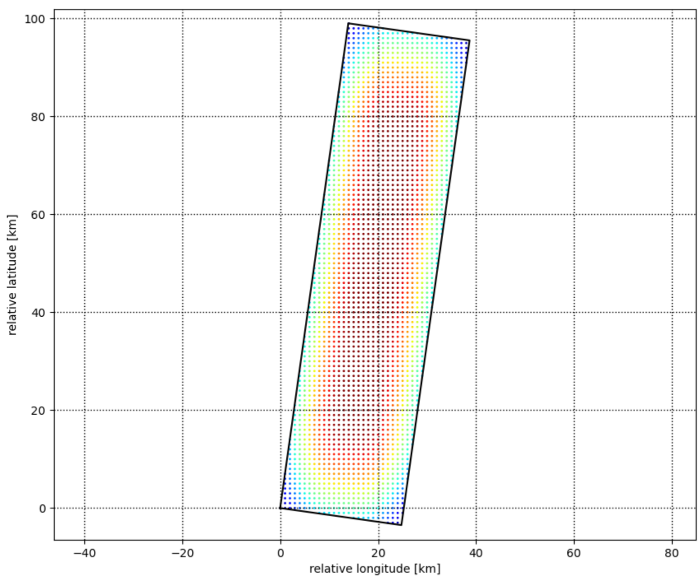

Fig.14 Feathering weights example. The product of range and azimuth weights is represented colour-coded.

4.1.4.2. Aggregation rule

The aggregation at pixel map level of the various L2a forest height maps is done by performing an average weighted by quality information represented by the percentage bias h_b^i, computed in sec. 3.5.4.1.6. The estimation quality h_b^i allows the combination of K different estimates H_F^i in a simple and efficient way to generate a global H_F estimate. A heat map *HM* is also stored as representing the sum of weights used in computation (including feathering weights). Two different sets of relations are proposed, depending on the availability of FD L2b product as input. When FD L2b product is not present, annotated forest/non-forest map is used to remove deforested areas:

$$H_F = \frac{\sum_{i=1}^{K} \frac{1}{\varepsilon + h_b^i} w_a^i(d) w_r^i(d) H_F^i FNF^{\,i}}{\sum_{i=1}^{K} \frac{1}{\varepsilon + h_b^i} w_a^i(d) w_r^i(d)} \tag{4.3}$$

$$h_b = \frac{\sum_{i=1}^{K} \frac{1}{\varepsilon + h_b^i} w_a^i(d) w_r^i(d) h_b^i FNF^{\,i}}{\sum_{i=1}^{K} \frac{1}{\varepsilon + h_b^i} w_a^i(d) w_r^i(d)}$$

$$HM = \sum_{i=1}^{K} \frac{1}{\varepsilon + h_b^i} w_a^i(d) w_r^i(d) FNF^{\,i}$$

where $\varepsilon = 0.01$ is an adjustment factor.

If the FD L2b product is provided as input, *CFM* supersedes *FNF*, and the rule is instead:

$$H_F = CFM \frac{\sum_{i=1}^{K} \frac{1}{\varepsilon + h_b^i} w_\mathrm{a}^i(d) w_\mathrm{r}^i(d) H_F^i}{\sum_{i=1}^{K} \frac{1}{\varepsilon + h_b^i} w_\mathrm{a}^i(d) w_\mathrm{r}^i(d)}$$

$$h_b = CFM \frac{\sum_{i=1}^{K} \frac{1}{\varepsilon + h_b^i} w_\mathrm{a}^i(d) w_\mathrm{r}^i(d) h_b^i}{\sum_{i=1}^{K} \frac{1}{\varepsilon + h_b^i} w_\mathrm{a}^i(d) w_\mathrm{r}^i(d)}$$

$$HM = CFM \sum_{i=1}^{K} \frac{1}{\varepsilon + h_b^i} w_\mathrm{a}^i(d) w_\mathrm{r}^i(d) \tag{4.4}$$

It must be noted that previous relations are actually computed only where at least one FH L2A input is present.